Received: 29 April 2020 | Revised: 5 February 2021 | Accepted: 18 February 2021

DOI: 10.1111/bph.15427

RESEARCH PAPER

# Activation of thyroid hormone receptor-β improved disease activity and metabolism independent of body weight in a mouse model of non-alcoholic steatohepatitis and fibrosis

Aimo Kannt[1,2,3] | Paulus Wohlfart[1] | Andreas Nygaard Madsen[4] | Sanne Skovgård Veidal[4] | Michael Feigh[4] | Dieter Schmoll[1]

[1]Diabetes Research, Sanofi Research and Development, Frankfurt, Germany

[2]Institute of Pharmacology, Goethe University, Frankfurt, Germany

[3]Department of Drug Discovery, Fraunhofer Institute for Translational Medicine and Pharmacology ITMP, Frankfurt, Germany

[4]NASH CRO, Gubra, Hørsholm, Denmark

**Correspondence**
Aimo Kannt Head of Drug Discovery
Fraunhofer Institute for Translational Medicine and Pharmacology Industriepark Hoechst, G879D-65926 Frankfurt/M., Germany
Email: aimo.kannt@itmp.fraunhofer.de

[Correction added on 22 April 2021, after first online publication: Corresponding author's address has been updated in this current version.]

**Background and Purpose:** Activation of hepatic thyroid hormone receptor β (THR-β) is associated with systemic lipid lowering, increased bile acid synthesis, and fat oxidation. In patients with non-alcoholic steatohepatitis (NASH), treatment with THR-β agonists decreased hepatic steatosis and circulating lipids, and induced resolution of NASH. We chose resmetirom (MGL-3196), a liver-directed, selective THR-β agonist, as a prototype to investigate the effects of THR-β activation in mice with diet-induced obesity (DIO) and biopsy-confirmed advanced NASH with fibrosis.

**Experimental Approach:** C57Bl/6J mice were fed a diet high in fat, fructose, and cholesterol for 34 weeks, and only biopsy-confirmed DIO-NASH mice with fibrosis were included. Resmetirom was administered at a daily dose of 3 $mg \cdot kg^{-1}$ p.o., for 8 weeks. Systemic and hepatic metabolic parameters, histological non-alcoholic fatty liver disease (NAFLD) activity and fibrosis scores, and liver RNA expression profiles were determined to assess the effect of THR-β activation.

**Key Results:** Treatment with resmetirom did not influence body weight but led to significant reduction in liver weight, hepatic steatosis, plasma alanine aminotransferase activity, liver and plasma cholesterol, and blood glucose. These metabolic effects translated into significant improvement in NAFLD activity score. Moreover, a lower content of α-smooth muscle actin and down-regulation of genes involved in fibrogenesis indicated a decrease in hepatic fibrosis.

**Conclusion and Implications:** Our model robustly reflected clinical observations of body weight-independent improvements in systemic and hepatic metabolism including anti-steatotic activity.

KEYWORDS
liver fibrosis, NASH, non-alcoholic steatohepatitis, resmetirom, thyroid hormone receptor

**Abbreviations:** ALT, alanine aminotransferase; AMLN diet, Amylin Liver NASH diet; AST, aspartate aminotransferase; DIO, diet-induced obesity; FDR, false-discovery rate; NAFLD, non-alcoholic fatty liver disease; NAS, NAFLD activity score; NASH, non-alcoholic steatohepatitis; PC, principal component; PCA, principal component analysis; SMA, smooth muscle actin; THR, thyroid hormone receptor.

[Correction added on 22 April 2021, after first online publication: Corresponding author's address has been updated in this current version.]

## 1 | INTRODUCTION

Non-alcoholic fatty liver disease (NAFLD) describes a spectrum of liver abnormalities ranging from fatty liver or simple steatosis to non-alcoholic steatohepatitis (NASH) without or with hepatic fibrosis. NAFLD is a common condition, with a global prevalence of approximately 25%, strongly linked to obesity, diabetes, and systemic dyslipidaemia (Younossi et al., 2016). NASH is characterized by marked hepatic steatosis, lobular inflammation and hepatocyte ballooning (Diehl & Day, 2017). The prevalence of NASH is increasing (Estes, Anstee, et al., 2018; Estes, Razavi, et al., 2018), and NASH with advanced fibrosis is associated with a strong increase in liver-related and overall mortality (Dulai et al., 2017; Ekstedt et al., 2015). No pharmacological therapy is approved for the treatment of NASH, though some experimental drugs are currently in later stages of clinical development (Garber, 2019). First-line therapy is lifestyle intervention with a focus on weight loss (Chalasani et al., 2018). Thus, new therapies for advanced NASH with fibrosis are urgently needed.

The **thyroid hormone receptor β (THR-β)** is the most abundant THR isoform in the liver but is also expressed in other tissues. Its expression in the liver is reduced in patients with NASH (Krause et al., 2018). Activation of hepatic THR-β is associated with systemic lipid lowering, increased bile acid synthesis and fat oxidation (Sinha et al., 2019). Liver-directed agonists with high selectivity for THR-β over **THR-α** have been generated (Erion et al., 2007; Kelly et al., 2014) and have shown metabolic benefits in preclinical models of diabetes and obesity, including reduced hepatic steatosis and inflammation (Sinha et al., 2019). However, there is little information on their activity in obese animals with manifest NASH and fibrosis. Recently, resmetirom (MGL-3196) was evaluated in a 36-week clinical phase 2 study in patients with biopsy-confirmed NASH, was well tolerated, and led to a significant reduction in hepatic fat fraction, circulating LDL cholesterol and triglycerides, and a higher rate of NASH resolution, compared to placebo (Harrison et al., 2019).

Here, we report the evaluation of resmetirom as a prototype of a liver-directed, selective THR-β agonist in a diet-induced obese (DIO) and biopsy-confirmed mouse model of advanced NASH with fibrosis. This is, to our knowledge, the first study describing the effects of resmetirom in a preclinical model of NASH, fully replicating recent clinical observations.

### What is already known

- Resmetirom reduces hepatic steatosis in patients with non-alcoholic steatohepatitis (NASH).
- Thyroid hormone receptor β (THR- β) agonists lower hepatic lipids in models of metabolic disease.

### What this study adds

- Resmetirom improves liver histopathology in diet-induced obese mice with NASH without causing weight loss.
- Whole genome expression analysis indicates activation of canonical THR-β signalling pathways and down-regulation of fibrogenesis.

### What is the clinical significance

- Long-term resmetirom treatment may lead to resolution of hepatic fibrosis.

## 2 | METHODS

### 2.1 | Animals

All animal care and experimental procedures were conducted according to the international principles for care and use of laboratory animals and were covered by personal licenses for Jacob Jelsing (2013-15-2934-00784 and 2015-15-0201-00518) issued by the Danish committee for animal research. Animal studies are reported in compliance with the ARRIVE guidelines (Percie du Sert et al., 2020) and with the recommendations made by the *British Journal of Pharmacology* (Lilley et al., 2020).

Thirty-six male C57BL/6J mice (5 weeks old), obtained from JanVier (JanVier Labs, France), were included in the study. Before treatment with resmetirom, animals had ad libitum access for 34 weeks to a regular rodent diet ($n$ = 12; Altromin 1324) or a diet high in fat (40%), of these 18% trans-fat, 40% carbohydrates (20% fructose), and 2% cholesterol ($n$ = 24; ) previously described as the Amylin Liver NASH diet (AMLN diet) (Clapper et al., 2013) and tap water. Mice were group housed at five animals per cage (UNO Plastic cages Type 3 for group housing, 427 × 267 mm, floor area 840 $cm^2$) under a 12/12-h dark–light cycle (lights off at 3 pm). Room temperature was controlled to 22°C ± 1°C, with 50% ± 10% humidity. Bedding was obtained from Brogaarden (cat. no. 30938).

### 2.2 | Preparation of model and study design

The effects of THR-β activation were investigated in mice with diet-induced obesity and biopsy-confirmed NASH and fibrosis (DIO-NASH model), as described earlier by Kristiansen et al. (2016). The study design is illustrated in Figure 1a. A baseline liver biopsy was conducted 3 weeks before the intervention for histological assessment of individual fibrosis (stage ≥1) and steatosis (score ≥2), as described (Kristiansen et al., 2016). After the baseline biopsy,

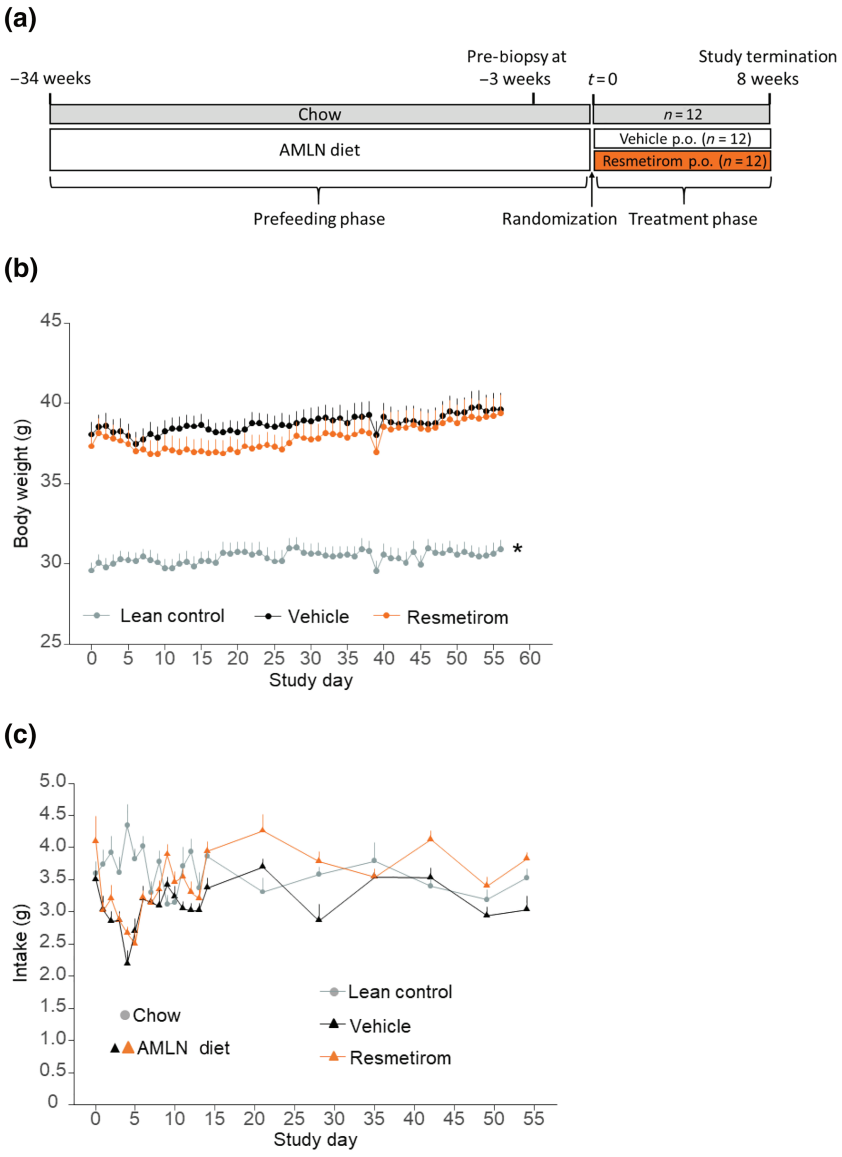


**FIGURE 1** (a) Study design. (b) Body weight development over the intervention period. (c) Food intake over the course of the study. $N = 12$ per group, $N = 11$ for vehicle control group. $^{*}P < .05$, significantly different from DIO-NASH vehicle control

animals were single housed (UNO Plastic cages Type 1 L Cage for single caging, 300 × 120 mm, floor area 360 $cm^2$) and remained so until the end of the study. A week before the intervention, the animals were randomized into groups of equal size and stratified according to liver Col1a1 quantification into three groups: Group 1, lean-chow control ($n$ = 12); Group 2, DIO-NASH + vehicle ($n$ = 12); and Group 3, DIO-NASH + resmetirom ($n$ = 12). Group sizes were selected based on previous studies with other drugs in the same model (Tølbøl et al., 2018). Group 1 contained all animals that had been on the regular rodent chow diet, whereas mice on the AMLN diet were randomized to Groups 2 and 3. Resmetirom was administered once daily, in the morning, by oral gavage at a dose of 3 $mg \cdot kg^{-1}$. The vehicle used for compound formulation and control injections was 0.6% methyl cellulose with 0.5% Tween 80. The resmetirom concentration in the dosing solution was 0.6 $mg \cdot ml^{-1}$; injection volume was 5 $ml \cdot kg^{-1}$ body weight. The intervention lasted for a period of 8 weeks. The DIO-NASH mice in the vehicle control and resmetirom groups remained on the NASH-inducing AMLN diet throughout the intervention period. At the end of the intervention, animals were killed in the fed state by heart puncture under isoflurane anaesthesia, and liver tissue and plasma were collected. One animal from the vehicle control group showed abnormal morphology in the portal tract on study termination and was therefore excluded from further analyses.

The dose of 3 $mg \cdot kg^{-1}$ was selected based on the dose–response to resmetirom (MGL-3196) on cholesterol lowering in DIO mice (Kelly et al., 2014). For mice with a body weight of 38 g (Figure 1b), this would correspond to a human equivalent dose of about 19 mg for an 80-kg person (Nair & Jacob, 2016) which is about four times lower than the dose of 80 mg used in a recent phase 2 study in NASH patients (Harrison et al., 2019). Thus, it can be assumed that resmetirom was not overdosed in our study, though the relationship between exposure profile and target engagement is not known and may be different across species.

Body weight determination, body composition analysis, blood sampling, plasma biochemistry, endotoxin determination and liver tissue biochemistry were performed in a blinded fashion as previously described (Kristiansen et al., 2016).

## 2.3 | Histological analyses

For histology, baseline liver biopsy and terminal samples were collected from the left lateral lobe (about 50–100 mg at baseline and 200 mg at the end) and fixed overnight in 4% paraformaldehyde. Liver tissue was paraffin embedded and sectioned (3-μm thickness). Sections were stained with haematoxylin and eosin and Sirius Red to assess hepatic steatosis and fibrosis, respectively, followed by analysis with Visiomorph software (Visiopharm, Denmark). Collagen 1α1 (col1a1), α-smooth muscle actin (α-SMA), and galectin-3 (gal-3) were assessed by quantitative immunohistochemistry staining using anti-col1a1 (RRID:AB_2753206, 1:300; Southern Biotech, Birmingham; catalogue number 1310-01, lot B2918-A688, IgG; secondary antibody Bright Vision anti-goat, ImmunoLogic, Netherlands), anti-α-SMA (RRID:AB_11129103, 1:800; Abcam, Cambridge, UK; catalogue number ab124964, lot #124973, IgG, clone EPR5368; secondary antibody Envision rabbit, Agilent Technologies, Glostrup, Denmark), or anti-gal-3 (RRID:AB_1134238; 1:50,000; BioLegend, San Diego, USA; catalogue number 125402, lot B160879, IgG2a, clone M3/38; secondary antibody anti-rat IgG 1:800, VWR, Soeborg, Denmark) as described (Kristiansen et al., 2016). The Immuno-related procedures used comply with the recommendations made by the *British Journal of Pharmacology* (Alexander et al., 2018). Antibodies were diluted in 5% pig serum; solutions were used only once. A pathologist blinded to the study performed the histological assessment and scoring. NAFLD activity score (NAS) combining steatosis, lobular inflammation, and hepatocyte ballooning scores and fibrosis stage were quantified applying the criteria proposed by Kleiner et al. (2005).

## 2.4 | RNA sequencing (gene expression analysis)

Liver tissue was harvested from the left lateral lobe, stabilized overnight in RNAlater® solution (Merck KGaA, Darmstadt, Germany) and stored at −80°C. Total RNA isolation was performed with the RNeasy kit following the instructions of the manufacturer (QIAGEN GmbH, Hilden, Germany). Quantity and integrity of purified RNA were measured with an Agilent RNA 6000 Nano kit using an Agilent 2100 Bioanalyzer (Agilent Technologies Inc, Waldbronn, Germany). Paired-end sequencing was performed using a TruSeq mRNA Library Kit (Illumina, San Diego, CA, USA) at Atlas Biolabs, Berlin, Germany, with a sequencing depth of 80 to 100 million reads per sample. RNA sequencing raw data were analysed using a software package and standardized RNA Seq analysis workflow (Array Studio Version 10.1.3.3, Omicsoft Qiagen). This workflow included alignment to a reference mouse gene model, quantification, normalization, and finally detection of differentially expressed genes using the DESeq2 module (RRID:SCR_015687; Costa-Silva et al., 2017).

## 2.5 | Data and statistical analyses

For all experiments, statistical analysis was only undertaken if group or sample size was at least $n = 5$, with group size referring to the number of independent values and not technical replicates. All available data were included in the analysis without removal of potential outliers. The data and statistical analysis comply with the recommendations of the *British Journal of Pharmacology* on experimental design and analysis in pharmacology (Curtis et al., 2018). Values of body weight, body composition analysis, blood sampling, plasma biochemistry, endotoxin determination and liver tissue biochemistry were analysed by one-way ANOVA with Dunnett's test. Data from histology and immunohistochemical analyses were assessed for differences in the number of animals showing improvement or worsening, using a one-sided Fisher's exact test with Bonferroni correction with the DIO-NASH vehicle group as comparator. Results from the gene expression analysis were corrected for variable multiplicity and false-discovery rate (FDR)-adjusted $P$ values calculated, using the Benjamini–Hochberg correction (Benjamini & Hochberg, 1995). Differentially expressed gene data were further interrogated on pathways and further causal relationships through the use of Ingenuity Pathway Analysis (RRID:SCR_008653, Ingenuity Qiagen) as described in Krämer et al. (2014). For all statistical analyses, $P$ values below 0.05 were considered to indicate significant differences between groups.

## 2.6 | Materials

Resmetirom (MGL-3196; catalogue no. HY-12216) was purchased from MedChemExpress (Hycultec GmbH, Beutelsbach, Germany). The control rodent diet Altromin 1324 was supplied by Brogaarden, (Lynge, Denmark) and the AMLN diet (D09100301) by Research Diets (New Brunswick, NJ, USA).

## 2.7 | Nomenclature of targets and ligands

Key protein targets and ligands in this article are hyperlinked to corresponding entries in the IUPHAR/BPS Guide to PHARMACOLOGY (http://www.guidetopharmacology.org) and are permanently archived in the Concise Guide to PHARMACOLOGY 2019/20 (Alexander, Cidlowski et al., 2019; Alexander, Fabbro et al., 2019; Alexander et al., 2019a, b).

# 3 | RESULTS

Figure 1b shows the change in body weight over the treatment period of 8 weeks. Resmetirom had no effect on weight or food

intake (Figure 1c) and was well tolerated throughout the treatment period with no obvious adverse effects or signs of toxicity. Body weight remained stable throughout the treatment period. The transient weight loss observed at day 39 in all three groups resulted from the 4-h fasting period before taking blood for glucose determination.

Activation of THR-β had a profound effect on plasma transaminase activities, leading to a reduction by about 50% for alanine aminotransferase (ALT) and 26% for aspartate aminotransferase (AST), compared with the DIO-NASH group treated with vehicle controls (Figure 2a,b). Plasma total cholesterol levels that were strongly elevated in DIO-NASH mice, compared with lean controls, were nearly normalized upon treatment with resmetirom (Figure 2c). There was a trend towards lower plasma triglycerides that was, however, not statistically significant (Figure 2d). Four-hour fasting blood glucose levels determined on treatment day 39 were significantly lower in resmetirom-treated animals (Figure 2e) whereas resmetirom had no influence on plasma insulin concentration (Figure 2f).

Liver hypertrophy observed in DIO-NASH mice was markedly reduced upon treatment with the THR-β agonist (Figure 3a), accompanied by a strong reduction in liver triglycerides, total cholesterol, and hepatic total lipid content (Figure 3b–d). Liver col1a1, α-SMA, and gal-3 contents were lower after resmetirom treatment (Figure 4). The difference from vehicle-treated DIO-NASH mice remained statistically significant upon normalization to liver weight for α-SMA, but not for col1a1 (not shown).

Resmetirom treatment was associated with changes in liver morphology (Figure 5a,b) and a significant improvement (post-treatment vs. pretreatment biopsy) in the histological NAS, relative

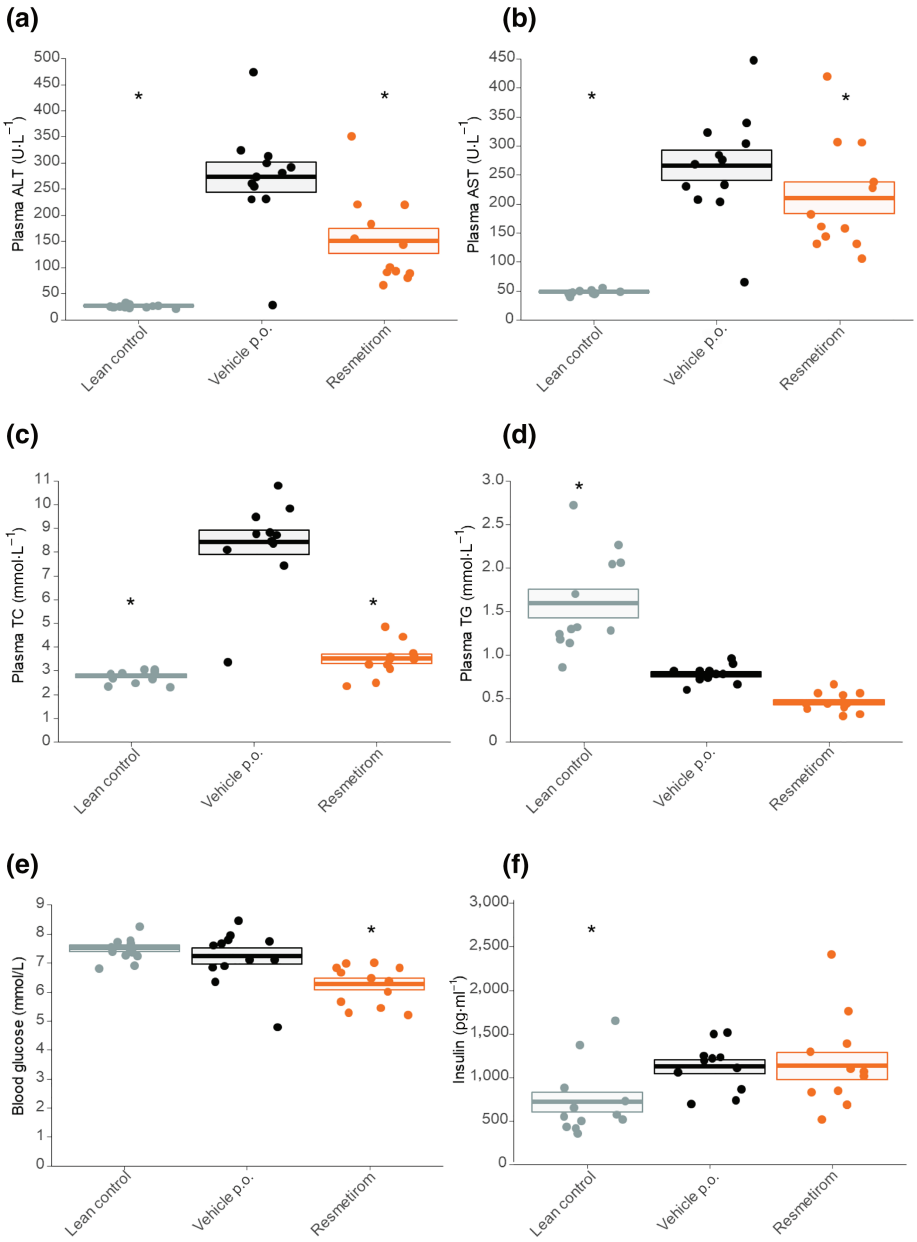


**FIGURE 2** Systemic safety and metabolic parameters. (a) Plasma ALT and (b) plasma AST activities. (c) Plasma total cholesterol, (d) plasma triglycerides, (e) 4-h fasting blood glucose, and (f) plasma insulin levels. (a)–(d) were measured at study termination, and (e) and (f) on study day 39. $N$ = 12 per group. Data shown are individual values with means ± SEM (shown as box). *$P$ < .05, significantly different from DIO-NASH vehicle control

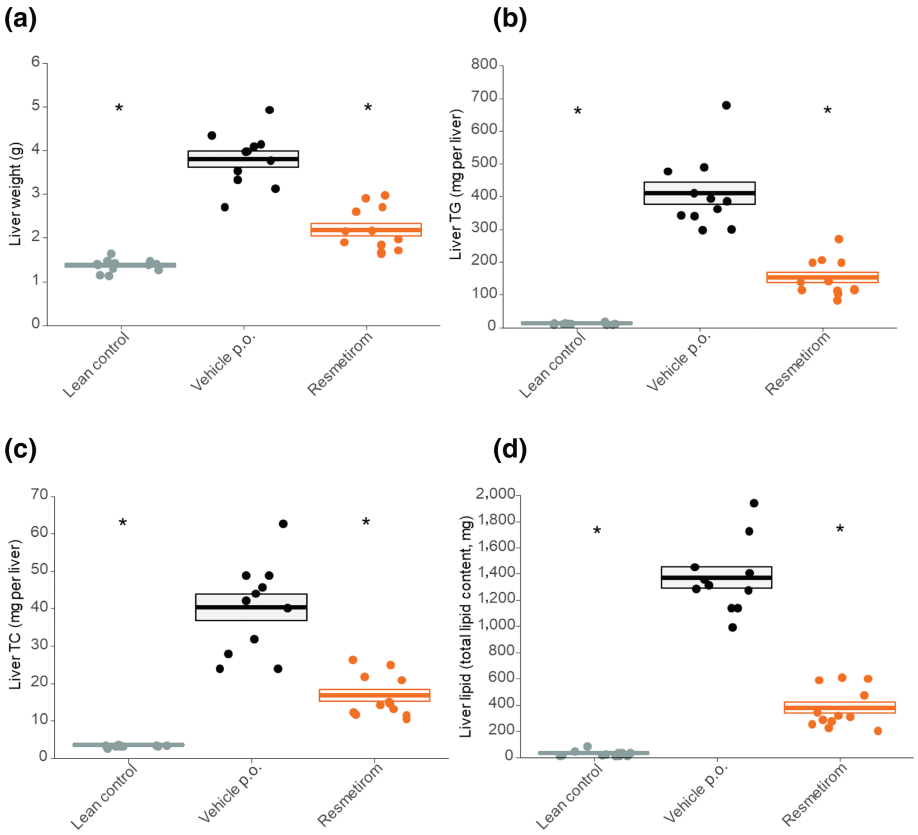


**FIGURE 3** Liver weight, hepatic lipid, collagen, and α-smooth muscle actin (α-SMA) content at study termination. (a) Wet liver weight, (b) hepatic triglycerides, and (c) hepatic total cholesterol. (d) Total liver lipid content. $N = 12$ per group, $N = 11$ for vehicle control group. Data shown are individual values with means ± SEM (shown as box). *$P < .05$, significantly different from DIO-NASH vehicle control

to DIO-NASH mice not exposed to the drug (Figure 5c). Whereas in DIO-NASH controls, two out of 11 mice had a lower NAS after the intervention period, 10 out of 12 resmetirom-treated mice showed an improved NAS (Figure 5c), in seven cases by more than one point. The individual scores of steatosis, lobular inflammation, and hepatocyte ballooning are shown in Figure S1. Whereas there was little to no change in steatosis and inflammation scores for the DIO-NASH vehicle control, a decrease in steatosis and inflammation score was seen for five out of 12 and eight out of 12 mice on resmetirom, respectively. Hepatocyte ballooning was not very pronounced in DIO-NASH mice. Fibrosis staging (pre-post) was lower in two out of 12 mice on resmetirom whereas no change was observed in vehicle-treated DIO-NASH control mice (difference not statistically significant; Figure 5d). There was no difference in Picrosirius staining fractional area between vehicle and resmetirom-treated mice (Figure S2).

Results of hepatic gene expression analysis by RNASeq are summarized in Figure 6. In a principal component analysis (PCA) of global gene expression, DIO-NASH vehicle-treated animals separated from lean control animals along the first two principal components (PC1 and PC2), with resmetirom treatment leading to a separation along PC2 towards values observed in lean control mice (Figure 6a). Among 53,431 transcripts assessed by RNA sequencing, DIO-NASH vehicle-treated mice demonstrated a >1.5-fold up-regulation of 4,614 genes (Figure S3a) in comparison to lean control animals. Only a fraction of these up-regulated genes (112 of 4,614) was significantly reversed by treatment with resmetirom (Figure S3b and Table S1). Furthermore, DIO-NASH vehicle-treated mice demonstrated a differential down-regulation (>1.5-fold) of 1,750 genes in comparison with lean control mice, with 79 of these transcripts being significantly reversed by resmetirom treatment. Notably, pathway analysis confirmed that changes in gene expression upon resmetirom treatment are consistent with THR-β activation (Figure 6b). Compared to DIO-NASH vehicle control animals, THR-β target genes such as deiodinase 1 (Dio1), malic enzyme 1 (Me1), cytochrome P450 7A1 (Cyp7a1), and glycerolphosphate dehydrogenase 2 (Gpd2) were found to be strongly up-regulated (Figure 6c). Lower expression of fibrosis marker genes collagen 1α1 (Col1a1), α-SMA (Acta2), lysyl oxidase-like 2 (Loxl2), and hydroxysteroid 17-β dehydrogenase 13 (Hsd17b13; Figure 6d) indicates a decrease in incident fibrogenesis which is also reflected in lower col1a1 and α-SMA protein levels (Figure 4a,b), although not enough to significantly improve the histological fibrosis staging (Figure 5d) within the observed treatment period. Other genes that were recently identified as markers of hepatic fibrosis or hepatocellular carcinoma such as LPS-binding protein (Lbp; Nien et al., 2018), ATP-binding cassette C3 (Abcc3; Carrasco-Torres et al., 2016), and fatty acid-binding protein 4 (Fabp4; Thompson et al., 2018) were markedly down-regulated upon treatment with resmetirom (Figure 6e). Of note, genes related to fatty acid synthesis (Acaca, Acacb, Fasn), lipolysis (Pnpla2, Lipe, Mgll), and fatty acid oxidation (Cpt1a, Pgc1a, Hadhb) were not found to be regulated upon resmetirom treatment compared with vehicle-treated DIO-NASH mice (Figure S4).

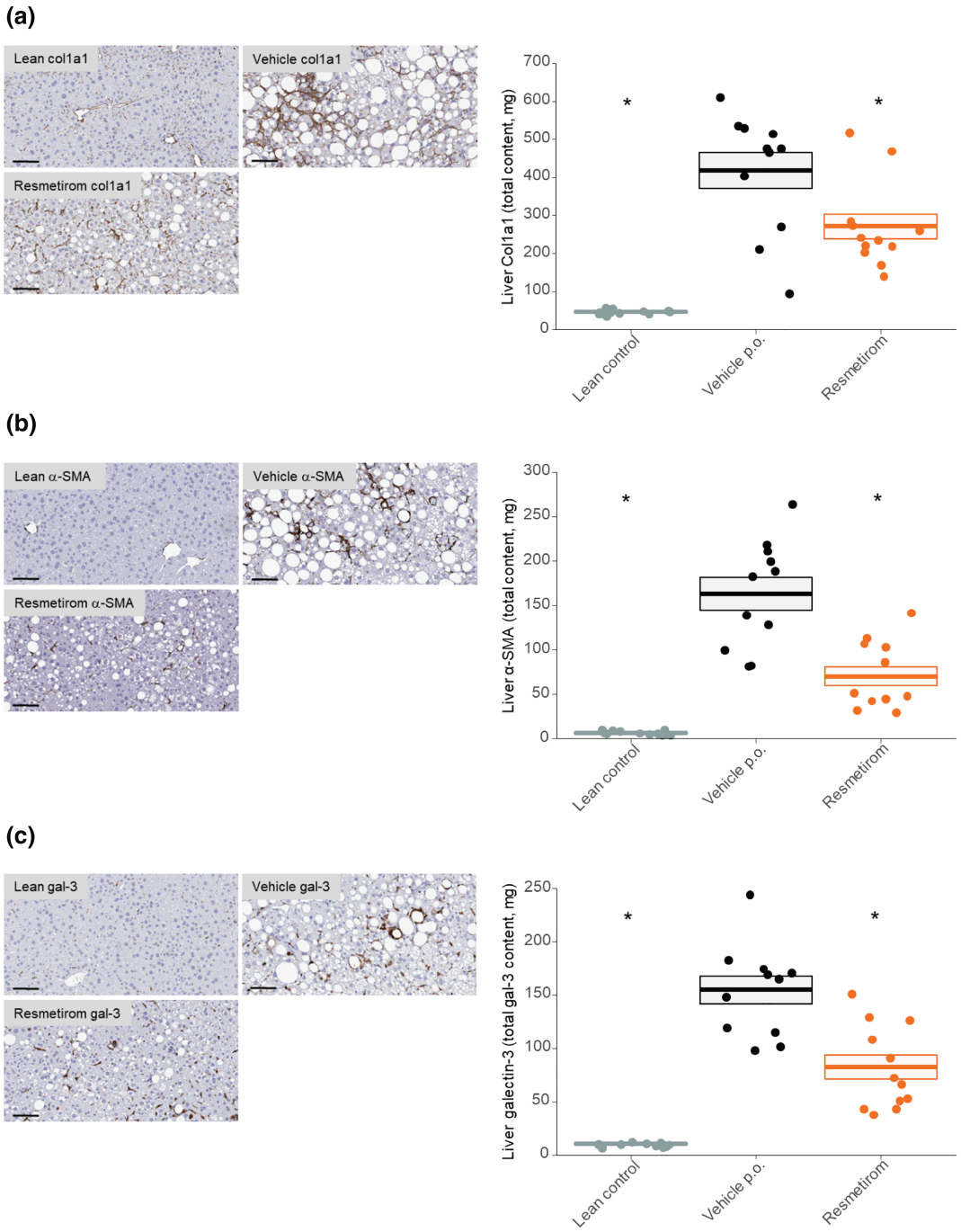


**FIGURE 4** Representative immunohistochemistry images and quantitative analysis of (a) hepatic collagen 1α1, (b) liver α-SMA, and (c) liver galectin-3. The length of the scale bar is 85 μm. $N = 12$ per group, $N = 11$ for vehicle control group. Data shown are individual values with means ± SEM (shown as box). *$P < .05$, significantly different from DIO-NASH vehicle control

## 4 | DISCUSSION

Here, we report that the liver-selective THR-β agonist resmetirom, administered at a dose that did not influence body weight or food intake, had a profound effect on hepatomegaly, hepatic steatosis, liver injury, circulating cholesterol, and the histological NAS in a DIO and biopsy-confirmed mouse model of advanced NASH with fibrosis. Our study was performed as an intervention (therapeutic) study in DIO-NASH mice with established metabolic disease also comprising obesity, hypercholesterolaemia, and insulin resistance, reflecting clinical characteristics of patients with NASH.

Our results are in very close agreement with a recently reported Phase II trial of resmetirom in patients with NASH in which, after 36 weeks of treatment, a 40% reduction in hepatic fat content measured by MRI was observed that was accompanied by a significant improvement in circulating liver transaminases, total and LDL

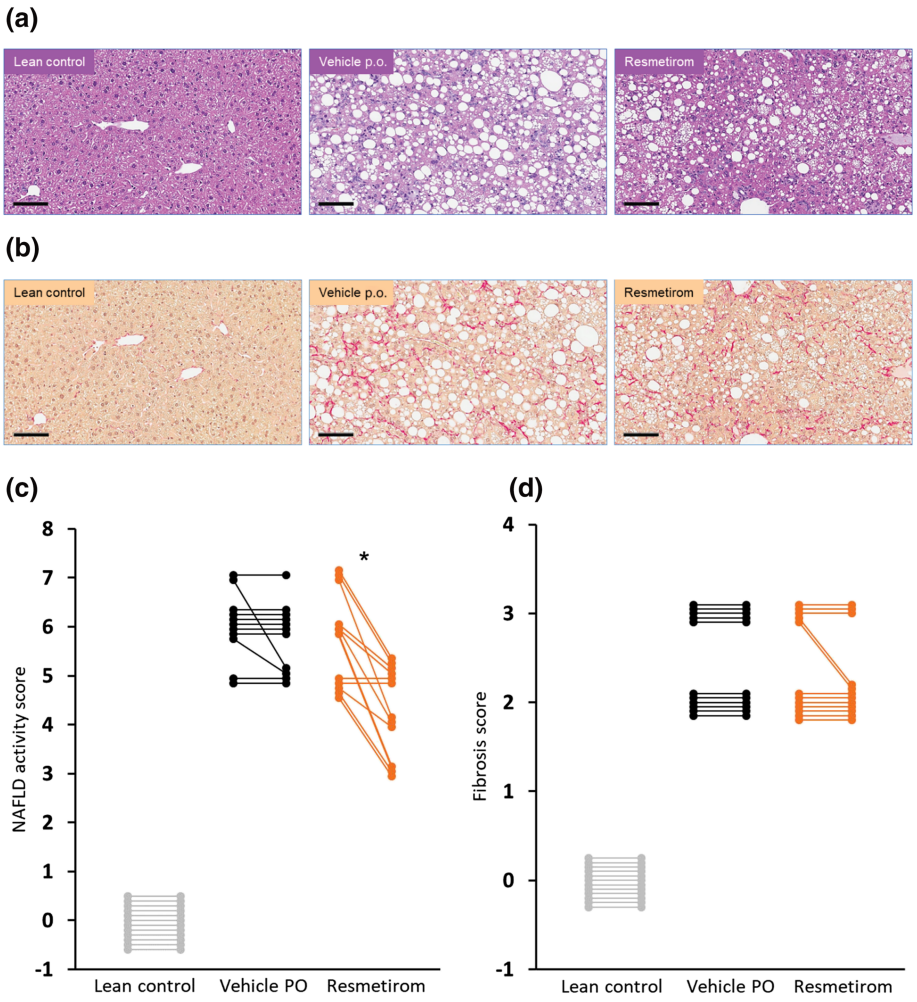


**FIGURE 5** (a) Representative images of liver morphology at termination of the study. H&E staining (20×, scale bar = 100 μm), (b) Sirius red staining (20×, scale bar = 100 μm). (c) Change in NAFLD activity score (pretreatment compared to post-treatment) for individual animals in the different treatment groups: Data shown are from lean control mice, DIO-NASH vehicle controls (Vehicle PO) and DIO-NASH mice treated with resmetirom (Resmetirom). (d) Change in fibrosis stage; data as in (c ). $N = 12$ per group, $N = 11$ for vehicle control group. $^{*}P < .05$, significantly different from DIO-NASH vehicle group; one-sided Fisher's exact test with Bonferroni correction

cholesterol. Furthermore, resmetirom responders that had lower hepatic fat fractions at 36 weeks also exhibited significantly reduced NASs (Harrison et al., 2019).

Several THR-β agonists have been investigated in animal models of metabolic disease with fatty liver (see Sinha et al., 2019). Sobetirome (GC-1) and eprotirome (KB2115), for example, reduced hepatic steatosis and liver triglycerides in ob/ob mice (Martagon et al., 2015). Notably, at the selected doses, treatment also resulted in significant body weight loss, and ob/ob mice do not develop manifest NASH or hepatic fibrosis under the investigated conditions. Similarly, both compounds, administered over a period of 10 days, led to strong reductions in liver triglyceride content in Sprague–Dawley rats on a high-fat diet (Vatner et al., 2013) that, however, did not develop NASH. Sobetirome also caused a marked decrease in hepatic and circulating triglycerides and serum ALT in rats fed a high-fat, methionine- and choline-deficient diet (Perra et al., 2008). However, treatment was accompanied by weight loss, and the presence of NASH was not investigated. MB07344/VK2809, a THR-β agonist prodrug selectively taken up by the liver and converted into the active form, reduced hepatic triglycerides and serum lipids in C57BL/6 mice on a high-fat diet and in Zucker diabetic fatty rats (Cable et al., 2009; Erion et al., 2007), in the absence of NASH and fibrosis. Thus, there is evidence from several models of metabolic disease for an improvement in liver fat and circulating lipids. Our results add to this body of evidence by showing that activation of THR-β can reduce hepatic steatosis and liver injury in a DIO model combining metabolic syndrome with advanced NASH and fibrosis.

Many preclinical models of NAFLD have been described that vary in their translatability to the human situation (Hansen et al., 2017). Our data indicate that with respect to THR-β agonists, data obtained in biopsy-confirmed DIO-NASH mice have a good human translatability. So far, it is not established to which extent resmetirom is able to also hold or to reverse fibrosis in late-stage NAFLD. In the recent Phase II trial of resmetirom in patients with NASH and predominantly mild fibrosis, no significant improvement was observed (Harrison et al., 2019). It is unclear whether this results from lack of efficacy or whether the treatment duration of 36 weeks was too short to elicit an observable improvement in hepatic fibrosis. Similar to the population investigated in this trial, our model showed mild fibrosis (approximately 60% F2, 40% F3; see Figure 5d), and no significant improvement in fibrosis score was seen with resmetirom. However, reduced expression of markers of fibrogenesis in resmetirom, compared with vehicle-treated DIO-NASH animals indicates an anti-fibrotic effect of THR-β activation that may translate into a more robust reduction in

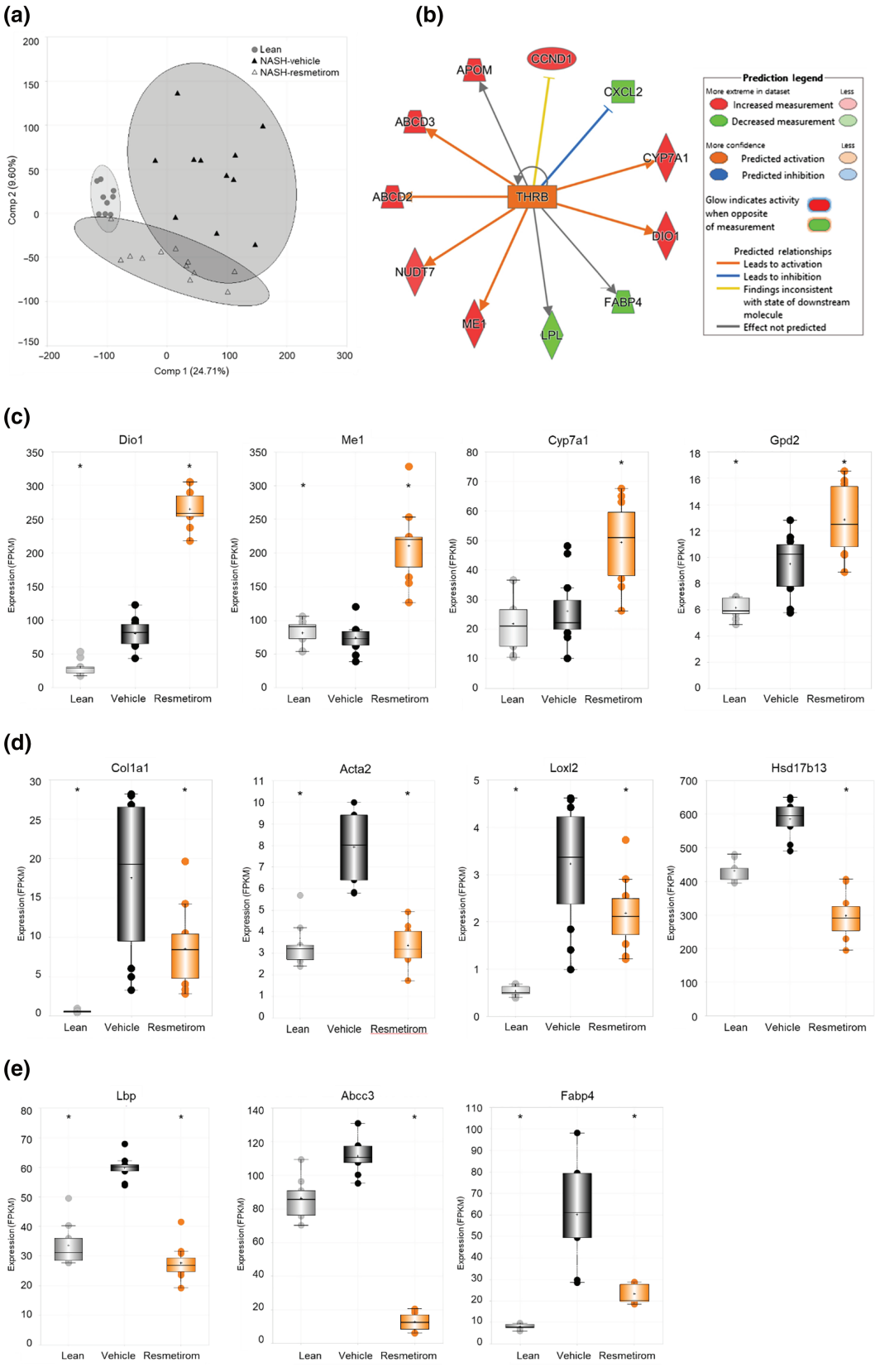


**FIGURE 6** Hepatic gene expression assessed by RNA sequencing with subsequent Ingenuity Pathway Analysis: (a) Principal component analysis over all 53,431 measured transcripts displaying the first two main components, PC1 and PC2. (b) Visualization of upstream factor analysis performed with Ingenuity, which predicts THR-β as one important factor activated in the resmetirom-treated group. (c–e) Expression of selected genes in normalized counts (FKPM) and shown as box-whisker blots with median (line) and mean (+) and confidence intervals of 5% to 95%. *$P$ < .05, significantly different from DIO-NASH vehicle group (false-discovery rate adjusted for multiplicity by Benjamini–Hochberg correction)

fibrosis upon longer duration of treatment. Thus, the 8-week treatment schedule in our study, chosen on the basis of previous studies in the same model with different types of intervention (Kannt et al., 2019, 2020; Tølbøl et al., 2018) may have been too short for a significant improvement in fibrosis score. Furthermore, as there was no worsening of fibrosis staging in the vehicle control group over the course of the intervention period (Figure 5b), prevention of fibrosis worsening by resmetirom could not be assessed. It is also possible that longer pre-feeding with the AMLN diet might further aggravate advanced fibrosis in DIO-NASH mice and could be a useful model for preclinical evaluation of the compound with respect to anti-fibrotic efficacy.

A drug for which an improvement in fibrosis has recently been observed is **obeticholic acid** (OCA): In a recently reported interim analysis of a Phase III trial, improvement of fibrosis by at least one stage, was seen in a significantly larger percentage of individuals treated with OCA, compared with placebo after 18 months (Younossi et al., 2019) which is about twice as long as the resmetirom Phase II trial (Harrison et al., 2019). In the DIO-NASH mouse model, OCA treatment over 8 weeks led, similarly to resmetirom in this study, to a reduction in expression of genes linked to fibrogenesis and a non-significant trend to an improvement in fibrosis score (Tølbøl et al., 2018). Thus, it is tempting to suggest that a longer treatment with OCA may also have translated into a more pronounced improvement in fibrosis in DIO-NASH mice or, likewise, longer treatment with resmetirom could lead to fibrosis improvement in patients.

Of note, although our whole genome expression analysis indicated activation of the canonical THR-β pathway, the data did not explain the strong reduction of hepatic lipids by resmetirom, as there was no clear down-regulation of fatty acid synthesis genes or stimulation of genes associated with fat oxidation. Thus, the anti-steatotic effect of the compound in this model is not due to transcriptional effects. It is possible that activation of THR-β redirects metabolic fluxes by post-transcriptional mechanisms.

An important limitation of our study is the restriction to a single dose level. The dose of 3 $mg \cdot kg^{-1}$ was selected based on a previous study in DIO mice over 23 days where this dose led to ~60% reduction in circulating cholesterol levels (Kelly et al., 2014). Whereas the chosen dose of resmetirom showed a marked improvement in hepatic and systemic metabolic health, in the absence of obvious adverse effects, additional studies investigating a range of doses will be required to, for example, establish the maximal tolerated or minimally or maximally effective doses of resmetirom for the treatment of NASH.

## ACKNOWLEDGEMENT

Claire Kammermeier is gratefully acknowledged for excellent technical assistance.

## AUTHOR CONTRIBUTIONS

A.K. and A.N.M. designed the study. A.K., P.W., A.N.M., and S.S.V. performed experiments and analysed data. M.F. and D.S. analysed data. A.K. wrote the paper. All authors edited and approved the manuscript.

## DECLARATION OF TRANSPARENCY AND SCIENTIFIC RIGOUR

This Declaration acknowledges that this paper adheres to the principles for transparent reporting and scientific rigour of preclinical research as stated in the *BJP* guidelines for Design & Analysis, Immunoblotting and Immunochemistry, and Animal Experimentation and as recommended by funding agencies, publishers, and other organizations engaged with supporting research.

## CONFLICT OF INTERESTS

A.K., P.W., and D.S. are or were employees of Sanofi. A.N.M., S.S.V., and M.F. are employees of Gubra.

## DATA AVAILABILITY STATEMENT

The data that support the findings of this study are available from the corresponding author upon reasonable request. Some data may not be made available because of privacy or ethical restrictions.

## ORCID

*Aimo Kannt* https://orcid.org/0000-0002-5197-2286

## REFERENCES

Alexander, S. P. H., Cidlowski, J. A., Kelly, E., Mathie, A., Peters, J. A., Veale, E. L., Armstrong, J. F., Faccenda, E., Harding, S. D., Pawson, A. J., Sharman, J. L., Southan, C., Davies, J. A., Davies, J. A., & CGTP Collaborators. (2019). The Concise Guide to PHARMACOLOGY 2019/20: Nuclear hormone receptors. *British Journal of Pharmacology*, *176*(Suppl 1), S229–S246.

Alexander, S. P. H., Fabbro, D., Kelly, E., Mathie, A., Peters, J. A., Veale, E. L., Armstrong, J. F., Faccenda, E., Harding, S. D., Pawson, A. J., Sharman, J. L., Southan, C., Davies, J. A., & CGTP Collaborators. (2019). The Concise Guide to PHARMACOLOGY 2019/20: Enzymes. *British Journal of Pharmacology*, *176*(Suppl 1), S297–S396.

Alexander, S. P. H., Kelly, E., Mathie, A., Peters, J. A., Veale, E. L., Armstrong, J. F., Faccenda, E., Harding, S. D., Pawson, A. J., Sharman, J. L., Southan, C., Davies, J. A., & CGTP Collaborators. (2019a). THE CONCISE GUIDE TO PHARMACOLOGY 2019/20: Transporters. *British Journal of Pharmacology*, *176*, S397–S493. https://doi.org/10.1111/bph.14753

Alexander, S. P. H., Roberts, R. E., Broughton, B. R. S., Sobey, C. G., George, C. H., Stanford, S. C., Cirino, G., Docherty, J. R., Giembycz, M. A., Hoyer, D., Insel, P. A., Izzo, A. A., Ji, Y., MacEwan, D. J., Mangum, J., Wonnacott, S., & Ahluwalia, A. (2018). Goals and practicalities of immunoblotting and immunohistochemistry: A guide for submission to the *British Journal of Pharmacology*. *British Journal of Pharmacology*, *175*, 407–411.

Alexander, S. P. H., Kelly, E., Mathie, A., Peters, J. A., Veale, E. L., Faccenda, E., Harding, S. D., Pawson, A. J., Sharman, J. L., Southan, C., Buneman, O. P., Cidlowski, J. A., Christopoulos, A., Davenport, A. P., Fabbro, D., Spedding, M., Striessnig, J., Davies, J. A., & CGTP Collaborators. (2019b). THE CONCISE GUIDE TO PHARMACOLOGY 2019/20: Other Protein Targets. *British Journal of Pharmacology*, *176*, S1–S20. https://doi.org/10.1111/bph.14747

Benjamini, Y., & Hochberg, Y. (1995). Controlling the false discovery rate: A practical and powerful approach to multiple testing. *Journal of the Royal Statistical Society B*, *57*, 289–300.

Cable E. E., Finn P. D., Stebbins J. W., Hou J., Ito B. R., van Poelje P. D., Linemeyer D. L., Erion M. D. (2009). Reduction of hepatic steatosis in rats and mice after treatment with a liver-targeted thyroid hormone receptor agonist. *Hepatology*, *49*(2), 407–417. http://doi.org/10.1002/hep.22572

Carrasco-Torres, G., Fattel-Fazenda, S., López-Alvarez, G. S., García-Román, R., Villa-Treviño, S., & Vásquez-Garzón, V. R. (2016). The transmembrane transporter ABCC3 participates in liver cancer progression and is a potential biomarker. *Tumour Biology*, *37*, 2007–2014. https://doi.org/10.1007/s13277-015-3999-5

Chalasani, N., Younossi, Z., Lavine, J. E., Charlton, M., Cusi, K., Rinella, M., Harrison, S. A., Brunt, E. M., & Sanyal, A. J. (2018). The diagnosis and management of nonalcoholic fatty liver disease: Practice guidance from the American Association for the Study of Liver Diseases. *Hepatology*, *67*, 328–357. https://doi.org/10.1002/hep.29367

Clapper, J. R., Hendricks, M. D., Gu, G., Wittmer, C., Dolman, C. S., Herich, J., Athanacio, J., Villescaz, C., Ghosh, S. S., Heilig, J. S., Lowe, C., & Roth, J. D. (2013). Diet-induced mouse model of fatty liver disease and nonalcoholic steatohepatitis reflecting clinical disease progression and methods of assessment. *American Journal of Physiology - Gastrointestinal and Liver Physiology*, *305*, G483–G495. https://doi.org/10.1152/ajpgi.00079.2013

Costa-Silva, J., Domingues, D., & Lopes, F. M. (2017). RNA-Seq differential expression analysis: An extended review and a software tool. *PLoS ONE*, *12*, e0190152. https://doi.org/10.1371/journal.pone.0190152

Curtis, M. J., Alexander, S. P. H., Cirino, G., Docherty, J. R., George, C. H., Giembycz, M. A., Hoyer, D., Insel, P. A., Izzo, A. A., Ji, Y., MacEwan, D. J., Sobey, C. G., Stanford, S. C., Teixeira, M. M., Wonnacott, S., & Ahluwalia, A. (2018). Experimental design and analysis and their reporting II: Updated and simplified guidance for authors and peer reviewers. *British Journal of Pharmacology*, *175*, 987–993. https://doi.org/10.1111/bph.14153

Diehl, A. M., & Day, C. (2017). Cause, pathogenesis, and treatment of nonalcoholic steatohepatitis. *New England Journal of Medicine*, *377*, 2063–2072. https://doi.org/10.1056/NEJMra1503519

Dulai, P. S., Singh, S., Patel, J., Soni, M., Prokop, L. J., Younossi, Z., Sebastiani, G., Ekstedt, M., Hagstrom, H., Nasr, P., Stal, P., Wong, V. W. S., Kechagias, S., Hultcrantz, R., & Loomba, R. (2017). Increased risk of mortality by fibrosis stage in nonalcoholic fatty liver disease: Systematic review and meta-analysis. *Hepatology*, *65*, 1557–1565. https://doi.org/10.1002/hep.29085

Ekstedt, M., Hagström, H., Nasr, P., Fredrikson, M., Stal, P., Kechagias, S., & Hultcrantz, R. (2015). Fibrosis stage is the strongest predictor for disease-specific mortality in NAFLD after up to 33 years of follow-up. *Hepatology*, *61*, 1547–1554. https://doi.org/10.1002/hep.27368

Erion, M. D., Cable, E. E., Ito, B. R., Jiang, H., Fujitaki, J. M., Finn, P. D., Zhang, B.-H., Hou, J., Boyer, S. H., van Poelje, P. D., & Linemeyer, D. L. (2007). Targeting thyroid hormone receptor-β agonists to the liver reduces cholesterol and triglycerides and improves the therapeutic index. *Proceedings of the National Academy of Sciences of the United States of America*, *104*, 15490–15495. https://doi.org/10.1073/pnas.0702759104

Estes, C., Anstee, Q. M., Arias-Loste, M. T., Bantel, H., Bellentani, S., Caballeria, J., Colombo, M., Craxi, A., Crespo, J., Day, C. P., Eguchi, Y., Geier, A., Kondili, L. A., Kroy, D. C., Lazarus, J. V., Loomba, R., Manns, M. P., Marchesini, G., Nakajima, A., … Razavi, H. (2018). Modeling NAFLD disease burden in China, France, Germany, Italy, Japan, Spain, United Kingdom, and United States for the period 2016–2030. *Journal of Hepatology*, *69*, 896–904. https://doi.org/10.1016/j.jhep.2018.05.036

Estes, C., Razavi, H., Loomba, R., Younossi, Z., & Sanyal, A. J. (2018). Modeling the epidemic of nonalcoholic fatty liver disease demonstrates an exponential increase in burden of disease. *Hepatology*, *67*, 123–133. https://doi.org/10.1002/hep.29466

Garber, K. (2019). The new liver epidemic. *Nature Biotechnology*, *37*, 209–214. https://doi.org/10.1038/s41587-019-0047-9

Hansen, H. H., Feigh, M., Veidal, S. S., Rigbolt, K. T., Vrang, N., & Fosgerau, K. (2017). Mouse models of nonalcoholic steatohepatitis in preclinical drug development. *Drug Discovery Today*, *22*, 1707–1718. https://doi.org/10.1016/j.drudis.2017.06.007

Harrison, S. A., Bashir, M. R., Guy, C. D., Zhou, R., Moylan, C. A., Frias, J. P., Alkhouri, N., Bansal, M. B., Baum, S., Neuschwander-Tetri, B. A., Taub, R., & Moussa, S. E. (2019). Resmetirom (MGL-3196) for the treatment of non-alcoholic steatohepatitis: A multicentre, randomised, double-blind, placebo-controlled, phase 2 trial. *The Lancet*, *394*, 2012–2024. https://doi.org/10.1016/S0140-6736(19)32517-6

Kannt, A., Madsen, A. N., Kammermeier, C., Elvert, R., Klöckener, T., Bossart, M., Haack, T., Evers, A., Lorenz, K., Hennerici, W., Rocher, C., Böcskei, Z., Guillemot, J. C., Mikol, V., Pattou, F., Staels, B., & Wagner, M. (2020). Incretin combination therapy for the treatment of non-alcoholic steatohepatitis. *Diabetes, Obesity and Metabolism*, *22*, 1328–1338. https://doi.org/10.1111/dom.14035

Kannt, A., Papada, E., Kammermeier, C., D'Auria, G., Jiménez-Hernández, N., Stephan, M., Schwahn, U., Madsen, A. N., Østergaard, M. V., Dedoussis, G., & Francino, M. P. (2019). Mastiha (*Pistacia lentiscus*) improves gut microbiota diversity, hepatic steatosis, and disease activity in a biopsy-confirmed mouse model of advanced non-alcoholic steatohepatitis and fibrosis. *Molecular Nutrition and Food Research*, *63*, e1900927.

Kelly, M. J., Pietranico-Cole, S., Larigan, J. D., Haynes, N. E., Reynolds, C. H., Scott, N., Vermeulen, J., Dvorozniak, M., Conde-Knape, K., Huang, K. S., So, S. S., Thakkar, K., Qian, Y., Banner, B., Mennona, F., Danzi, S., Klein, I., Taub, R., & Tilley, J. (2014). Discovery of 2-[3,5-dichloro-4-(5-isopropyl-6-oxo-1,6-dihydropyridazin-3-yloxy) phenyl]-3,5-dio xo-2,3,4,5-tetrahydro[1,2,4]triazine-6-carbonitrile (MGL-3196), a highly selective thyroid hormone receptor β agonist in clinical trials for the treatment of dyslipidemia. *Journal of Medicinal Chemistry*, *57*, 3912–3923. https://doi.org/10.1021/jm4019299

Kleiner, D. E., Brunt, E. M., Van Natta, M., Behling, C., Contos, M. J., Cummings, O. W., Ferrell, L. D., Liu, Y.-C., Torbenson, M. S., Unalp-Arida, A., Yeh, M., McCullough, A. J., Sanyal, A. J., & Nonalcoholic Steatohepatitis Clinical Research Network. (2005). Design and validation of a histological scoring system for nonalcoholic fatty liver disease. *Hepatology*, *41*, 1313–1321. https://doi.org/10.1002/hep.20701

Krämer, A., Green, J., Pollard, J. Jr., & Tugendreich, S. (2014). Causal analysis approaches in Ingenuity Pathway Analysis. *Bioinformatics*, *30*, 523–530. https://doi.org/10.1093/bioinformatics/btt703

Krause, C., Grohs, M., El Gammal, A. T., Wolter, S., Lehnert, H., Mann, O., Mittag, J., & Kirchner, H. (2018). Reduced expression of thyroid hormone receptor β in human nonalcoholic steatohepatitis. *Endocrine Connections*, *7*, 1448–1456. https://doi.org/10.1530/EC-18-0499

Kristiansen, M. N., Veidal, S. S., Rigbolt, K. T., Tølbøl, K. S., Roth, J. D., Jelsing, J., Vrang, N., & Feigh, M. (2016). Obese diet-induced mouse models of nonalcoholic steatohepatitis-tracking disease by liver biopsy. *World Journal of Hepatology*, *8*, 673–684. https://doi.org/10.4254/wjh.v8.i16.673

Lilley, E., Stanford, S. C., Kendall, D. E., Alexander, S. P. H., Cirino, G., Docherty, J. R., George, C. H., Insel, P. A., Izzo, A. A., Ji, Y., Panettieri, R. A., Sobey, C. G., Stefanska, B., Stephens, G., Teixeira, M., & Ahluwalia, A. (2020). ARRIVE 2.0 and the *British Journal of Pharmacology*: Updated guidance for 2020. *British Journal of Pharmacology*, *177*, 3611–3616. https://doi.org/10.1111/bph.15178

Martagon, A. J., Lin, J. Z., Cimini, S. L., Webb, P., & Phillips, K. J. (2015). The amelioration of hepatic steatosis by thyroid hormone receptor agonists is insufficient to restore insulin sensitivity in ob/ob mice. *PLoS ONE*, *10*, e0122987. https://doi.org/10.1371/journal.pone.0122987

Nair A. B., Jacob S. (2016). A simple practice guide for dose conversion between animals and human. *Journal of Basic and Clinical Pharmacy*, *7* (2), 27. http://doi.org/10.4103/0976-0105.177703

Nien, H. C., Sheu, J. C., Chi, Y. C., Chen, C. L., Kao, J. H., & Yang, W. S. (2018). One-year weight management lowers lipopolysaccharide-binding protein and its implication in metainflammation and liver fibrosis. *PLoS ONE*, *13*, e0207882. https://doi.org/10.1371/journal.pone.0207882

Percie du Sert, N., Hurst, V., Ahluwalia, A., Alam, S., Avey, M. T., Baker, M., Browne, W. J., Clark, A., Cuthill, I. C., Dirnagl, U., Emerson, M., Garner, P., Holgate, S. T., Howells, D. W., Karp, N. A., Lazic, S. E., Lidster, K., MacCallum, C. J., Macleod, M., … Würbel, H. (2020). The ARRIVE guidelines 2.0: Updated guidelines for reporting animal research. *PLoS Biology*, *18*(7), e3000410. https://doi.org/10.1371/journal.pbio.3000410

Perra, A., Simbula, G., Simbula, M., Pibiri, M., Kowalik, M. A., Sulas, P., Cocco, M. T., Ledda-Columbano, G. M., & Columbano, A. (2008). Thyroid hormone (T3) and TRβ agonist GC-1 inhibit/reverse nonalcoholic fatty liver in rats. *The FASEB Journal*, *22*, 2981–2989. https://doi.org/10.1096/fj.08-108464

Sinha, R. A., Bruistroop, E., Singh, B. K., & Yen, P. M. (2019). Nonalcoholic fatty liver disease and hypercholesterolemia: Roles of thyroid hormones, metabolites, and agonists. *Thyroid*, *29*, 1173–1191. https://doi.org/10.1089/thy.2018.0664

Thompson, K. J., Austin, R. G., Nazari, S. S., Gersin, K. S., Iannitti, D. A., & McKillop, I. H. (2018). Altered fatty acid-binding protein 4 (FABP4) expression and function in human and animal models of hepatocellular carcinoma. *Liver International*, *38*, 1074–1083. https://doi.org/10.1111/liv.13639

Tølbøl, K. S., Kristiansen, M. N., Hansen, H. H., Veidal, S. S., Rigbolt, K. T., Gillum, M. P., Jelsing, J., Vrang, N., & Feigh, M. (2018). Metabolic and hepatic effects of liraglutide, obeticholic acid and elafibranor in diet-induced obese mouse models of biopsy-confirmed nonalcoholic steatohepatitis. *World Journal of Gastroenterology*, *24*, 179–194. https://doi.org/10.3748/wjg.v24.i2.179

Vatner, D. F., Weismann, D., Beddow, S. A., Kumashiro, N., Erion, D. M., Liao, X. H., Grover, G. J., Webb, P., Phillips, K. J., Weiss, R. E., Bogan, J. S., Baxter, J., Shulman, G. I., & Samuel, V. T. (2013). Thyroid hormone receptor-β agonists prevent hepatic steatosis in fat-fed rats but impair insulin sensitivity via discrete pathways. *American Journal of Physiology - Endocrinology and Metabolism*, *305*, E89–E100. https://doi.org/10.1152/ajpendo.00573.2012

Younossi, Z. M., Koenig, A. B., Abdelatif, D., Fazel, Y., Henry, L., & Wymer, M. (2016). Global epidemiology of nonalcoholic fatty liver disease—Meta-analytic assessment of prevalence, incidence, and outcomes. *Hepatology*, *64*, 73–84. https://doi.org/10.1002/hep.28431

Younossi, Z. M., Ratziu, V., Loomba, R., Rinella, M., Anstee, Q. M., Goodman, Z., Bedossa, P., Geier, A., Beckebaum, S., Newsome, P. N., Sheridan, D., Sheikh, M. Y., Trotter, J., Knapple, W., Lawitz, E., Abdelmalek, M. F., Kowdley, K. V., Montano-Loza, A. J., Boursier, J., … Zuin, M. (2019). Obeticholic acid for the treatment of non-alcoholic steatohepatitis: Interim analysis from a multicentre, randomised, placebo-controlled phase 3 trial. *The Lancet*, *394*, 2184–2196. https://doi.org/10.1016/S0140-6736(19)33041-7

## SUPPORTING INFORMATION

Additional supporting information may be found online in the Supporting Information section at the end of this article.

**How to cite this article:** Kannt A, Wohlfart P, Madsen AN, Veidal SS, Feigh M, Schmoll D. Activation of thyroid hormone receptor-β improved disease activity and metabolism independent of body weight in a mouse model of non-alcoholic steatohepatitis and fibrosis. *Br J Pharmacol*. 2021; 178:2412–2423. https://doi.org/10.1111/bph.15427